ARTICLES
PUBLISHED ONLINE: 16 AUGUST 2009 | DOI: 10.1038/NPHYS1366
nature physics

Locking electron spins into magnetic resonance by electron–nuclear feedback

Ivo T. Vink, Katja C. Nowack, Frank H. L. Koppens, Jeroen Danon, Yuli V. Nazarov and Lieven M. K. Vandersypen*

Quantum information processing requires accurate coherent control of quantum-mechanical two-level systems, but is hampered in practice by their coupling to an uncontrolled environment. For electron spins in III–V quantum dots, the random environment is mostly given by the nuclear spins in the quantum-dot host material; they collectively act on the electron spin through the hyperfine interaction, much like a random magnetic field. Here we show that the same hyperfine interaction can be harnessed such that partial control of the normally uncontrolled environment becomes possible. In particular, we observe that the electron-spin-resonance frequency remains locked to the frequency of an applied microwave magnetic field, even when the external magnetic field or the excitation frequency are changed. The nuclear field thereby adjusts itself such that the electron-spin-resonance condition remains satisfied. General theoretical arguments indicate that this spin-resonance locking might be accompanied by a significant reduction of the randomness in the nuclear field.

Individual electron spins in semiconductor quantum dots are attractive for applications in quantum information processing, as demonstrated by the considerable progress that has been made towards this goal[1]. Nearly all experiments in this direction have been realized in III–V materials where all isotopes carry nuclear spin. In thermodynamic equilibrium, the nuclear spins in the quantum dot host material are randomly oriented, even at dilution refrigerator temperatures and in magnetic fields of a few Tesla. An electron spin confined in the quantum dot interacts through the hyperfine coupling with $N \sim 10^6$ nuclear spins and as a result experiences a random nuclear field B_N. This random nuclear field is sampled from a distribution with a root mean square width $\propto IA/g\mu_B\sqrt{N}$, where g is the electron g factor, μ_B the Bohr magneton, I the nuclear spin and A the hyperfine coupling constant ($IA \approx 135\,\mu$eV in GaAs). Measurements typically give a width of $\sim$1 mT. As a result, we lose track of the phase of a freely evolving electron spin within a time T_2^* of a few tens of nanoseconds[2–6]. Similarly, when the spin evolves under an oscillating driving field, the nuclear field leads to a random offset in the resonance condition that has an amplitude comparable to that of currently achievable driving fields. This results in poorly controlled spin rotations[7].

It is therefore of great importance to develop the ability to control and manipulate the nuclear field with great precision. In particular, it would be highly desirable to set the nuclear field to a narrow distribution of values at the start of every experiment[8–11]. This would immediately reduce the rapid dephasing, and the electron spin would lose phase coherence only from the slow subsequent evolution of the nuclear field, giving a predicted spin coherence time of 1–10 μs (refs 12, 13). Such narrowing has been achieved in an ensemble of self-assembled quantum dots by synchronizing the precessing spins with a series of laser pulses[14]. Also, the spread of the difference in nuclear fields in two neighbouring quantum dots was reduced through a gate-voltage-controlled pumping cycle, giving a 70-fold increase in the T_2^* for states in the two-electron subspace with magnetic quantum number $m_z = 0$ (ref. 15).

Here we exploit electron–nuclear feedback to control and manipulate the nuclear fields in two coupled quantum dots during continuous wave (CW) driving of the electron spins in the dots. We observe that each nuclear field adjusts itself such that the electron spin in the corresponding quantum dot remains in resonance with a fixed driving frequency, even when we sweep the external magnetic field away from the nominal resonance condition. Similarly, the electron-spin-resonance (ESR) frequency remains locked to the excitation frequency when the excitation frequency is swept back and forth. These distinctive features set our observations apart from the many previous observations of dynamic nuclear spin polarization in quantum dots, in both transport[16–20] and optical measurements[21–23]. We investigate the origin of this feedback by studying its dependence on the amplitudes of the applied a.c. magnetic and electric fields and on the sweep rates. Furthermore, we show theoretically that the spin resonance locking must be accompanied by a narrowing of the nuclear-field distribution, in the present experiment by more than a factor of 10.

ESR detection scheme

The measurements are performed on an electrostatically defined double quantum dot tuned to the Pauli spin-blockade regime[24], with effectively one excess electron on each dot (the actual electron number is small but unknown). We measure the d.c. current through the double-quantum-dot device, which depends on the spin states of the electrons residing on the dots. When the two electrons have parallel spins, the electron flow through the dots is blocked. When one of the spins is flipped, the spin blockade is lifted and electrons flow through the two dots until the system returns to a state with parallel spins on the two dots. As previously demonstrated[7], it is possible to flip the electron spins through magnetic resonance, by a.c. excitation of an on-chip wire which generates an oscillating magnetic field at the dots: when the excitation frequency, f, matches the ESR frequency, $|g|\mu_B B_0/h$, a finite current flows through the device. Here h is Planck's constant, and B_0 the external magnetic field. In addition, current can flow at zero magnetic field, where the electron spins can flip–flop with the nuclear spins in the substrate[17]. We use this zero-field feature to determine and adjust for small magnetic-field offsets present

Kavli Institute of Nanoscience, Delft University of Technology, PO Box 5046, 2600 GA Delft, The Netherlands. *e-mail: l.m.k.vandersypen@tudelft.nl.

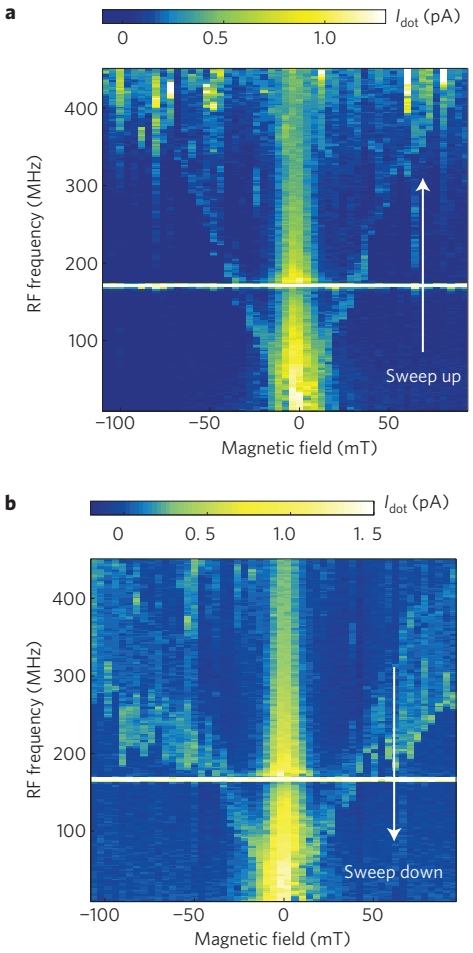

Figure 1 | ESR locking during frequency sweeps. a, Current through the double dot (colour scale) subject to CW magnetic excitation, when sweeping the frequency up at fixed magnetic fields. The bright fork indicates the position of the ESR condition. **b**, Similar to **a** but sweeping the frequency down. The ESR frequency remains locked to the excitation frequency when the excitation frequency is swept past the nominal resonance condition. The feature at 180 MHz is due to a resonance in the transmission line in our dilution refrigerator.

in our set-up. The zero-field peak and the ESR response are seen in current measurements under CW excitation with increasing excitation frequency at fixed magnetic fields (Fig. 1a), similar to the data published in ref. 7, and taken on the same device but in a different cooldown.

Locking to the spin-resonance condition

Surprisingly, when we reverse the sweep direction, a distinctly different behaviour is observed over a wide range of dot settings (see Supplementary Information for details of the tuning parameters). Current starts flowing when the driving frequency hits the spin-resonance frequency but remains high even as the frequency is swept well below the nominal resonance condition (Fig. 1b). The fact that the current remains high implies that the electron spin is still on resonance with the excitation frequency, and that an effective field, B_{eff}, counteracts the external magnetic field B_0: $hf = |g|\mu_{\mathrm{B}}(B_0 + B_{\mathrm{eff}})$. From the fact that the current is strongly reduced when we simultaneously excite any of the three nuclear spin species in the substrate (data not shown), we conclude that this effective field is created by dynamical nuclear-spin polarization, that is, $B_{\mathrm{eff}} = B_{\mathrm{N}}$. This nuclear field builds up at exactly the right rate to keep the electron spin in resonance with the changing

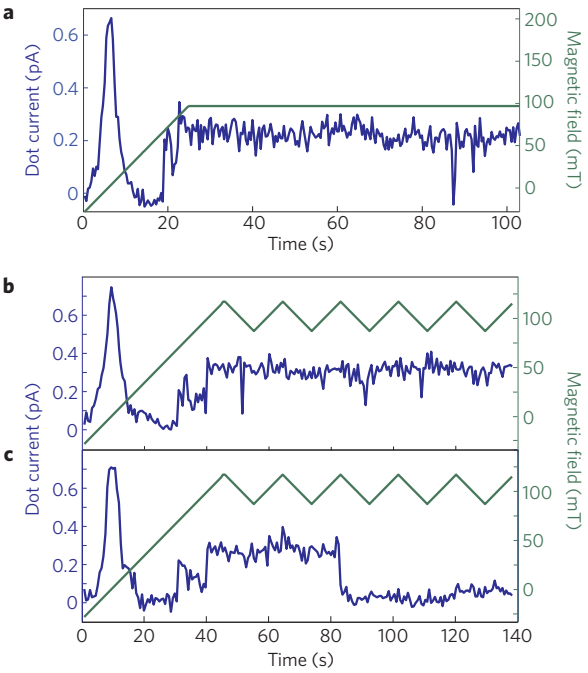

Figure 2 | ESR locking during magnetic-field sweeps. a, Current through the double dot as a function of time, while the magnetic field is first ramped up (right axis) and subsequently held fixed, under CW excitation ($f = 400$ MHz). **b**,**c**, Two current traces similar to **a**, but after the magnetic field is ramped up, it is repeatedly swept down and back up over a 30 mT range (right axis). After the ESR condition is first met, the electron spin remains locked into magnetic resonance for up to two minutes, even though the resonance condition is shifted back and forth.

driving frequency, which implies there is a built-in electron–nuclear feedback mechanism.

Similar dragging of the resonance is observed when sweeping the magnetic field for a fixed excitation frequency. In Fig. 2a we show typical data obtained from measurements where the magnetic field is swept from −33 to 97 mT (right vertical axis) in about 25 s. We first see the zero-field peak, as expected, and next the current jumps up around $B_0 = 67$ mT, which is slightly below the nominal resonance condition ($f = 400$ MHz, $|g| = 0.36$). The current remains high as the field is swept further to 97 mT, which is well outside the ESR linewidth in the absence of feedback (see Fig. 3b below). Similar to the case of the frequency sweeps, a nuclear field builds up in exactly such a way as to maintain the ESR frequency locked to the excitation frequency. When we subsequently keep the field fixed at 97 mT, we observe that the electron spin can remain locked into magnetic resonance for well over a minute.

It is even possible to drag the nuclear field back and forth under fixed-frequency excitation. In Fig. 2b,c, B_0 is ramped up from −33 to 117 mT, and is subsequently swept back and forth between 117 and 87 mT in a triangular pattern. The current again jumps up as we sweep through resonance and subsequently remains high independent of the sweep direction, implying that after the system is locked on resonance the sign of $\mathrm{d}B_0/\mathrm{d}t$ ($\mathrm{d}f/\mathrm{d}t$) does not matter as long as the condition $B_0 > B^{\mathrm{res}} = hf/g\mu_{\mathrm{B}}$ ($f < f^{\mathrm{res}} = g\mu_{\mathrm{B}}B_0/h$) remains fulfilled. In Fig. 2c the resonance is lost after approximately 1 min, whereas in Fig. 2b the spin remains locked on resonance during the entire experiment (about 2 min).

Locking characteristics

These remarkable observations of spin-resonance locking due to electron–nuclear feedback are characterized by a number of common features. First, the current jumps up abruptly, in many cases in

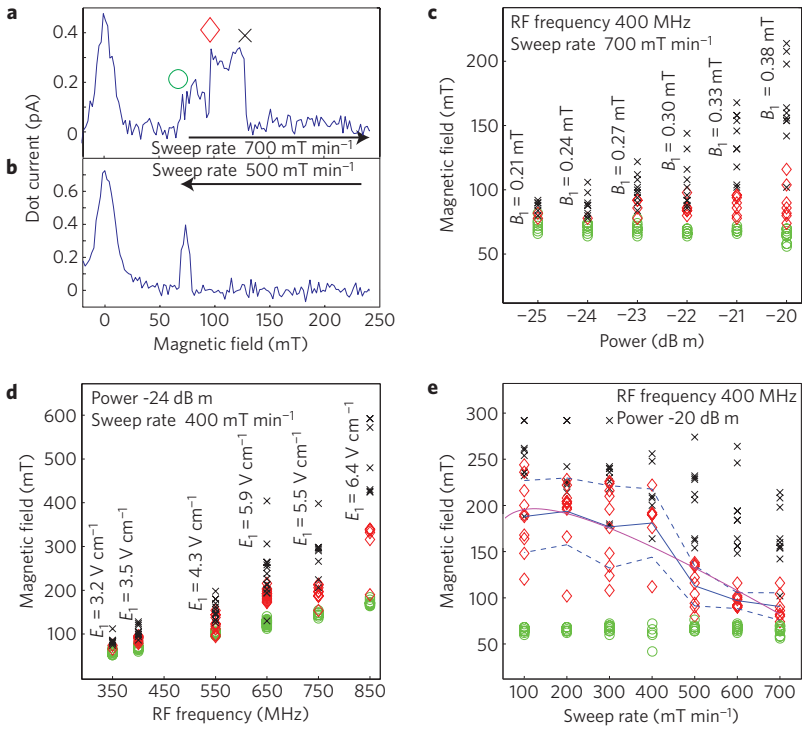

Figure 3 | ESR locking dependence on excitation power, frequency and sweep rate. a, Current through the double dot as the magnetic field is swept up ($f = 400$ MHz). **b**, Similar to **a** but now B_0 is swept down. No dragging effects are observed; the narrow peak gives the position of the nominal resonant field. **c**, Scatter plot of the switching fields as indicated by the symbols in **a** (for their definitions, see the main text), as a function of the power applied to the on-chip wire, obtained from multiple sweeps as in **a**. The corresponding resonant magnetic-field amplitude B_1 at the dot is given as well. **d**, Scatter plot similar to **c**, as a function of f. The electric field amplitude E_1 estimated from photon-assisted tunnelling generally increases with f, and is shown in the figure. **e**, Scatter plot similar to **c** as a function of magnetic-field sweep rate. Blue lines: average and standard deviation of the magnetic fields where the second current jump is observed. Purple curve: fit of these average values with a theoretical model (see Supplementary Information). We note that there is no build-up of B_N in the limit of zero sweep rate, so the predicted switching field first increases with sweep rate, before decreasing.

less than a few hundred milliseconds, at a field value that varies over 10–30 mT around the nominal resonance condition (see the green circles in Fig. 3 below). This is a further indication that the system is actively pulled into resonance—without feedback a current peak with smooth flanks and a width of a few millitesla is expected[25]. Second, the resonance dragging generally occurs only for fields larger than the nominal resonant field, or for frequencies lower than the nominal resonance frequency. This is opposite to the case of the usual Overhauser effect, as discussed further below. Third, the initial current jump is usually followed by a second current jump, before the current drops back to zero. A possible explanation for this double step is that the first current plateau corresponds to a situation where both dots are on resonance, and that only one dot remains on resonance after the second jump (see Supplementary Information for a discussion of the current levels). When the resonance is lost also in this second dot, the current returns to zero.

This interpretation of the double current step is supported by pump–probe measurements shown in Fig. 4. Starting from the second current plateau with $B_0 = 80$ mT and $f = 276$ MHz, we switch off the CW excitation and probe the position of the ESR frequency as the nuclear field returns to equilibrium (we use short bursts for probing to minimize feedback during the probe phase). We see that the ESR frequency returns to its nominal value, slightly above 400 MHz, within 20 s, corresponding to the relaxation time of the local nuclear spin polarization (white dashed line). This signal must originate from a dot that is still locked into magnetic resonance at the end of the pump phase. In addition, we see a response at the nominal resonance frequency already from the start of the probe phase (red dashed line). Presumably, this signal arises from the other dot, where the resonance was lost during the pump phase and the nuclear field has (nearly) relaxed by the time the probe phase starts.

Dependence on sweep and excitation parameters

To better understand the locking mechanism, we study how far the nuclear-spin polarization can be dragged by performing magnetic-field sweeps as a function of the applied microwave power, the microwave frequency and the magnetic-field sweep rate. Specifically, we repeatedly ramp the magnetic field from −28 mT upwards and record (1) the field at which the current jumps up (circle in Fig. 3a), (2) the field where the current jumps to a still higher value (diamond) and (3) the field where the current drops back to zero (cross). The resulting data points are shown as scatter plots in Fig. 3c–e, using the same symbols.

The first current jump always occurs as the nominal resonant field (in the absence of feedback) is first approached. The second jump and the current drop occur at fields that increase with driving amplitude over the range that we could explore (for still stronger driving, spin blockade was lifted by photon-assisted tunnelling so we lost sensitivity to spin flips). For the highest powers accessible in the experiment, the electron spin is maintained on resonance over a magnetic field range of a few 100 mT. As the power is reduced, the locking effect vanishes. Furthermore, the field that can be reached before the resonance is lost increases with excitation frequency. Earlier measurements on the same sample showed that along with the a.c. magnetic field an a.c. electric field is generated, whose amplitude for a fixed power (and magnetic field amplitude) increases roughly linearly with the excitation frequency[7]. The dependence on driving frequency can therefore also be interpreted as stronger locking for higher electric field amplitudes. Finally,

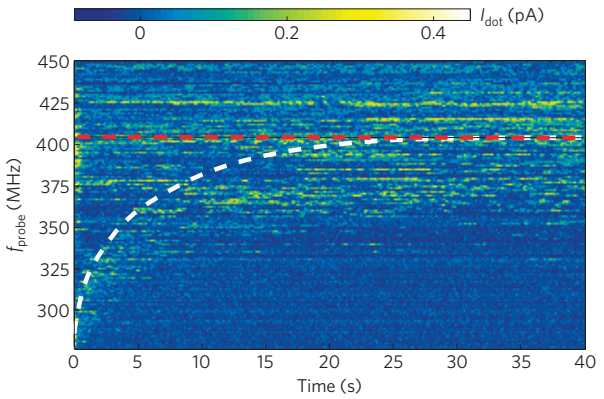

Figure 4 | Pump–probe measurement of the relaxation of the nuclear-spin polarization. At a fixed magnetic field of $B_0 = 80$ mT, we apply CW excitation (power $P = -13$ dB m), sweeping the frequency from 500 to 276 MHz at 43 MHz s^{-1}, and dragging the nuclear field along (pump phase). Next we turn off the CW excitation and record the current as a function of time while applying 140 ns microwave bursts every 2 μs at frequency f_{probe} (vertical axis) throughout a 40 s probe phase. As the nuclear-spin polarization relaxes, the resonance condition $|g|\mu_B(B_0 + B_N(t)) = hf_{probe}$ will be fulfilled at some point in time, at which the current sets on again. Varying f_{probe} then reveals the nuclear-spin relaxation as indicated by the white dashed line (guide to the eye) marking the onset of the current, where the probe pulses have had the least effect on the nuclear polarization. Even though the excitation is applied only in bursts, the electron spin nevertheless remains locked into resonance in some cases, stalling the nuclear-spin relaxation. The red dashed line marks an additional signal at the nominal resonance frequency already present from the start of the probe phase.

we see that for higher magnetic-field sweep rates the resonance is lost at lower fields.

A phenomenological rate-equation model

A few basic considerations give insight into the mechanism behind these observations. To describe the nuclear-spin dynamics we construct a rate-equation model directly from the experimental data. For clarity we discuss the nuclear-spin dynamics in one of the dots; the results for two dots are qualitatively similar[26] and the fact that the tunnel coupling is small (smaller than the typical nuclear field in equilibrium) justifies considering the electron spins as independent. First we describe in general terms a mechanism that explains the observed locking and the dragging of the nuclear polarization, and afterwards we turn to the origin of this mechanism.

The nuclear-spin polarization x in the dot is felt as an effective magnetic field by the electron spin: $IAx = g\mu_B B_N$ (x is defined as dimensionless, $-1 \leq x \leq 1$; in our experiments, $|x| \ll 1$). In the absence of any excitation, the polarization naturally relaxes to zero on a characteristic timescale τ_n, owing to nuclear-spin diffusion. However, the nuclear-spin dynamics will be altered by hyperfine-mediated electron–nuclear flip–flops when the electron spins are brought out of equilibrium[16–18]. In the spin-blockade regime at finite B_0, such non-equilibrium dynamics is induced when the electron spins are resonantly excited by an external microwave magnetic or electric field. This occurs when the nuclear polarization is close to x^{res} with $IAx^{res} = g\mu_B B_N^{res} = |g|\mu_B B_0 - hf$. Regardless of the relevant microscopic processes, we thus expect in very general terms a polarization-dependent pump rate $\Gamma_p(x - x^{res})$, which is non-zero only close to the resonance condition $x = x^{res}$. The dynamics of the polarization in the dot is then described by

$$\frac{dx}{dt} = \Gamma_p(x - x^{res}) - \frac{1}{\tau_n}x \qquad (1)$$

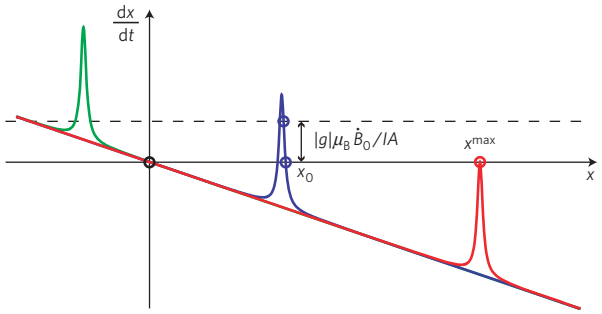

Figure 5 | Nuclear-spin pumping curves. The nuclear-spin polarization rate for one dot (dx/dt) is shown as a function of its polarization x for three different values of x^{res} (the green, blue and red curves). The overall negative slope is due to nuclear-spin relaxation and the resonant peak is due to the external driving. Circles indicate stable points in nuclear-spin polarization and are found whenever the curve crosses the x axis with a negative slope. During a field (or frequency) sweep, a dynamic equilibrium is reached where $dx/dt = |g|\mu_B\dot{B}_0/IA$.

where Γ_p peaks when its argument $(x - x^{res})$ is zero. Figure 5 qualitatively visualizes equation (1) in the form of a pumping curve for three different values of x^{res}, where we have (for now arbitrarily) chosen the resonant contribution to be positive. From the figure we can see that stable points of nuclear polarization occur when dx/dt crosses zero with a negative slope: if x is higher (lower) than the stable polarization x_0, dx/dt is negative (positive) and x gets pushed back to x_0. Owing to nuclear spin relaxation there is almost always a stable point at $x = 0$. Depending on the particular shape of Γ_p, hence on the specific experimental regime, there can be one or more additional stable points[26–28].

We now interpret the field-sweep experiments within this simple picture. First, given that the current remains high in field sweeps, a stable point must exist close to resonance, in agreement with our expectation of a resonant peak in Γ_p. Next, as dragging is generally observed only for $x > 0$, Γ_p must be positive, as in Fig. 5. Finally, from the maximum nuclear field B_N^{max} that can be achieved by dragging, we can estimate the height of Γ_p: when the maximum of the pumping peak falls below zero, that is, when nuclear spin relaxation exceeds the resonant pumping, the stable point at $x > 0$ disappears and B_N relaxes to zero (Fig. 5, red curve).

During actual field sweeps, at a rate $\dot{B}_0$, the resonance is lost at fields below B_N^{max}: as a dynamic equilibrium is reached when $dx/dt = |g|\mu_B\dot{B}_0/IA$ instead of $dx/dt = 0$, the stable operating point moves up the pumping curve (see Fig. 5) and disappears when the sweep rate exceeds the maximum of the pumping peak. In practice we will lose the resonance even earlier, because intrinsic nuclear field fluctuations can drive the nuclear field across the maximum. We model the average switching field taking into account such fluctuations by assuming an exponential dependence of the switching rate on the 'barrier height'. The result is illustrated in Fig. 4e. This combined picture captures very well the experimental observation that for higher sweep rates the resonance is more easily lost, but not at exactly the same field every time.

We next turn to the nature of the extrinsic pumping process, Γ_p. First, the stable points in the experiment generally occur for $x > 0$; that is, the nuclear field points against the external magnetic field. This is opposite to the usual Overhauser effect, where electron spins are excited by magnetic resonance and relax back from ↓ to ↑ by flip–flopping with the nuclear spins, thereby creating a nuclear polarization in the direction of the electron-spin excited state. The observed 'reverse' pumping is possible when there is an excess of ↑ electrons, which are excited to ↓ by resonant electric fields, whereby the nuclear spins absorb the angular momentum[28,29]. Spin relaxation in general creates an excess of ↑ electrons, which favours

reverse pumping. In our experiment, we believe the dominating electron-spin relaxation process to be spin exchange with the leads due to photon-assisted tunnelling (estimated to be 10–100 kHz). Second, the locking effect gets stronger, hence Γ_p becomes larger, not only with stronger driving in general (Fig. 3c), but also with stronger electric excitation by itself (higher f, Fig. 3d). On the basis of these observations, we suggest that electric-field-assisted electron–nuclear flip–flops combined with electron-spin relaxation are mainly responsible for the resonant pumping[26].

Implications for electron-spin dephasing

Finally, we analyse theoretically the implications of our observations for the width of the nuclear field distribution. We define $\Gamma_{\pm}(x)$ as the total positive and negative nuclear spin-flip rates that result from the intrinsic relaxation and resonant response combined, so $dx/dt = (2/N)(\Gamma_+ - \Gamma_-)$, where N denotes the total number of nuclei. We also define $\gamma(x)$ as the total rate of nuclear spin flips, $\gamma = (2/N)(\Gamma_+ + \Gamma_-)$. Using the fact that the pumping curve shows a resonant peak at $|x_0| \ll 1$, we can then approximate the variance of the nuclear polarization distribution around x_0 as (see Supplementary Information)

$$\sigma^2 \approx \frac{1}{N} \frac{\gamma(x_0)}{\left(-\frac{\partial}{\partial x}\frac{dx}{dt}\right)|_{x_0}} \qquad (2)$$

The numerator is the local diffusion rate, and the denominator is the restoring force—the steeper the slope of dx/dt, the stronger the restoring force. When labelling the number of nuclei with spin up (down) by $N_{+(-)}$ we get for the case without pumping $\Gamma_{\pm} = N_{\mp}/2\tau_n$, so equation (2) gives us the usual result $\sigma^2 = 1/N$. (Note that we assume here for simplicity nuclear spin $I = 1/2$; for higher values of spin, for example $I = 3/2$ as in GaAs, the results do not change qualitatively.) For a stable point $x_0 > 0$ near resonance, we take as a rough estimate for the local slope the maximum of Γ_p divided by its width. This gives $\sigma^2 \approx B_1/NB_N^{max}$ (see Supplementary Information). As B_N^{max} was several hundred millitesla with $B_1 < 1$ mT, these arguments imply that the nuclear field distribution was narrowed by more than a factor of 10. Future experiments will aim at a quantitative study of the impact of this narrowing on the electron-spin dephasing time through Ramsey-style experiments.

Narrowing of the nuclear-field distribution would greatly enhance our level of control of the electron-spin dynamics. Furthermore, the observed locking effect enables us to accurately set the spin-resonance frequency of an electron in a quantum dot to a value determined only by the externally controlled excitation frequency. Finally, our measurements suggest that we can selectively control the ESR frequency in one of the dots, which could be exploited for independent addressing of electron spins in quantum dots that are less than 100 nm apart.

Received 17 February 2009; accepted 10 July 2009; published online 16 August 2009

References

1. Hanson, R., Kouwenhoven, L. P., Petta, J. R., Tarucha, S. & Vandersypen, L. M. K. Spins in few-electron quantum dots. *Rev. Mod. Phys.* **79,** 1217–1265 (2007).
2. Khaetskii, A. V., Loss, D. & Glazman, L. Electron spin decoherence in quantum dots due to interaction with nuclei. *Phys. Rev. Lett.* **88,** 186802 (2002).
3. Merkulov, I. A., Efros, Al. L. & Rosen, M. Electron spin relaxation by nuclei in semiconductor quantum dots. *Phys. Rev. B* **65,** 205309 (2002).
4. Petta, J. R. *et al.* Coherent manipulation of coupled electron spins in semiconductor quantum dots. *Science* **309,** 2180–2184 (2005).
5. Koppens, F. H. L., Nowack, K. C. & Vandersypen, L. M. K. Spin echo of a single electron spin in a quantum dot. *Phys. Rev. Lett.* **100,** 236802 (2008).
6. Greilich, A. *et al.* Mode locking of electron spin coherences in singly charged quantum dots. *Science* **313,** 341–345 (2006).
7. Koppens, F. H. L. *et al.* Driven coherent oscillations of a single electron spin in a quantum dot. *Nature* **442,** 766–771 (2006).
8. Burkard, G., Loss, D. & DiVincenzo, D. P. Coupled quantum dots as quantum gates. *Phys. Rev. B* **59,** 2070–2078 (1999).
9. Klauser, D., Coish, W. A. & Loss, D. Nuclear spin state narrowing via gate-controlled Rabi oscillations in a double quantum dot. *Phys. Rev. B* **73,** 205302 (2006).
10. Giedke, G., Taylor, J. M., D'Alessandro, D., Lukin, M. D. & Imamoğlu, A. Quantum measurement of a mesoscopic spin ensemble. *Phys. Rev. A* **74,** 032316 (2006).
11. Stepanenko, D., Burkard, G., Giedke, G. & Imamoğlu, A. Enhancement of electron spin coherence by optical preparation of nuclear spins. *Phys. Rev. Lett.* **96,** 136401 (2006).
12. Coish, W. A. & Loss, D. Hyperfine interaction in a quantum dot: Non-Markovian electron spin dynamics. *Phys. Rev. B* **70,** 195340 (2004).
13. Witzel, W. M. & Das Sarma, S. Quantum theory for electron spin decoherence induced by nuclear spin dynamics in semiconductor quantum computer architectures: Spectral diffusion of localized electron spins in the nuclear solid-state environment. *Phys. Rev. B* **74,** 035322 (2006).
14. Greilich, A. *et al.* Collective single mode precession of electron spins in a quantum dot ensemble. *Phys. Rev. B* **79,** 201305(R) (2009).
15. Reilly, D. J. *et al.* Suppressing spin qubit dephasing by nuclear state preparation. *Science* **321,** 817–821 (2008).
16. Ono, K. & Tarucha, S. Nuclear-spin-induced oscillatory current in spin-blockaded quantum dots. *Phys. Rev. Lett.* **92,** 256803 (2004).
17. Koppens, F. H. L. *et al.* Control and detection of singlet–triplet mixing in a random nuclear field. *Science* **309,** 1346–1350 (2005).
18. Reilly, D. J. *et al.* Measurement of temporal correlations of the Overhauser field in a double quantum dot. *Phys. Rev. Lett.* **101,** 236803 (2008).
19. Foletti, S. *et al.* Dynamic nuclear polarization using a single pair of electrons. Preprint at <http://arxiv.org/abs/0801.3613> (2008).
20. Baugh, J., Kitamura, Y., Ono, K. & Tarucha, S. Large nuclear Overhauser fields detected in vertically coupled double quantum dots. *Phys. Rev. Lett.* **99,** 096804 (2007).
21. Tartakovskii, A. I. *et al.* Nuclear spin switch in semiconductor quantum dots. *Phys. Rev. Lett.* **98,** 026806 (2007).
22. Braun, P.-F. *et al.* Bistability of the nuclear polarization created through optical pumping in $In_{1-x}Ga_xAs$ quantum dots. *Phys. Rev. B* **74,** 245306 (2006).
23. Maletinsky, P., Lai, C. W., Badolato, A. & Imamoğlu, A. Nonlinear dynamics of quantum dot nuclear spins. *Phys. Rev. B* **75,** 035409 (2007).
24. Ono, K., Austing, D. G., Tokura, Y. & Tarucha, S. Current rectification by Pauli exclusion in a weakly coupled double quantum dot system. *Science* **297,** 1313–1317 (2002).
25. Koppens, F. H. L. *et al.* Detection of single electron spin resonance in a double quantum dot. *J. Appl. Phys.* **101,** 081706 (2007).
26. Danon, J. *et al.* Multiple nuclear polarization states in a double quantum dot. *Phys. Rev. Lett.* **103,** 046601 (2009).
27. Danon, J. & Nazarov, Yu. V. Nuclear tuning and detuning of the electron spin resonance in a quantum dot: Theoretical consideration. *Phys. Rev. Lett.* **100,** 056603 (2008).
28. Rudner, M. S. & Levitov, L. S. Electrically driven reverse Overhauser pumping of nuclear spins in quantum dots. *Phys. Rev. Lett.* **99,** 246602 (2007).
29. Laird, E. A. *et al.* Hyperfine-mediated gate-driven electron spin resonance. *Phys. Rev. Lett.* **99,** 246601 (2007).

Acknowledgements

We thank F. R. Braakman, P. C. de Groot, R. Hanson, M. Laforest, L. R. Schreiber, G. A. Steele and S.-C. Wang for help and discussions, and R. Schouten, A. van der Enden, R. G. Roeleveld and P. van Oossanen for technical support. This work is supported by the 'Stichting voor Fundamenteel Onderzoek der Materie (FOM)' and the 'Nederlandse Organisatie voor Wetenschappelijk Onderzoek (NWO)'.

Author contributions

I.T.V., K.C.N and F.H.L.K. performed the experiment, I.T.V., K.C.N., F.H.L.K. and L.M.K.V were responsible for the project planning, J.D. and Y.V.N. developed the theory, all authors contributed to the interpretation of the data and I.T.V., K.C.N, J.D. and L.M.K.V wrote the manuscript.

Additional information

Supplementary information accompanies this paper on www.nature.com/naturephysics. Reprints and permissions information is available online at http://npg.nature.com/reprintsandpermissions. Correspondence and requests for materials should be addressed to L.M.K.V.